

Overvoltage characteristics in symmetrical monopolar HB MMC-HVDC configuration comprising long cable systems

M. Goertz^{*,a}, S. Wenig^b, S. Beckler^{*,b}, C. Hirsching^a, M. Suriyah^a, T. Leibfried^a

^a Karlsruhe Institute of Technology (KIT), Institute of Electric Energy Systems and High Voltage Technology (IEH), Karlsruhe, BW 76131, Germany

^b TransnetBW GmbH, Stuttgart, BW 70191, Germany

ARTICLE INFO

Keywords:

Extruded dc cable system
Half-bridge
HVDC
Insulation co-ordination
OHL-cable mixed system

ABSTRACT

This contribution focuses on high voltage direct current (HVDC) transmission systems comprising modular multilevel converters (MMC) equipped with half-bridge (HB) submodules and analyses cable voltage stresses during various station internal as well as dc side faults. In order to examine relevant overvoltage characteristics affecting HVDC cable systems, a systematic approach to evaluate overvoltage stresses is presented and an extensive set of time-domain simulations is analysed for schemes operating in symmetrical monopolar configuration. Obtained results are relevant for considerations on insulation co-ordination of HVDC cable systems and for a comprehensive definition of high voltage testing requirements.

1. Introduction

The number of installed HVDC projects in symmetrical monopolar (SMP) configuration based on HB-MMC technology is emerging at a fast pace [1]. In line with the gathered project and operational experiences, several articles have covered the aspects of overvoltage stresses in SMP configuration caused by station internal or dc side faults. The general system behaviour under dc side faults is discussed in [2]. Studies concerning the insulation co-ordination of converter station equipment or focusing on cable overvoltages are conducted in [3] and [4–6], respectively. With regard to offshore projects, [7] reports on the gained operational experience and presents an overvoltage wave shape measured by a transient fault recorder during a cable fault. Moreover, recent research focuses on the laboratory imitation of representative overvoltage shapes during dc side faults in SMP configuration [8,9]. However, since standardized test levels for HVDC cable systems with extruded insulation are not yet available [10,11], preliminary insulation co-ordination studies are still of essential importance to provide a reliable design strategy applied to the cable system. This contribution analyses overvoltages affecting the cable system in case of very long land cable systems and gives an indication of the overvoltage characteristics in case of systems comprising mixed overhead lines (OHL) and cable sections. Compared to previously published papers [12,13] the focus of this contribution is laid on the build-up of the voltage wave shapes leading to the highest occurring crest values. Besides, the front-parameters of the overvoltage such as rise time and steepness are

discussed and additional case study results are provided for mixed systems operating in SMP configuration. The scope of this research is motivated by the designated HVDC links in Germany [14].

This paper is structured as follows. Section 2 describes the investigated HVDC systems in SMP configuration and outlines the underlying modelling method applied in EMT-software. Subsequently, Section 3 presents a systematic approach to evaluate voltage stresses occurring along the cable route. Section 4 focuses on schemes comprising solely cable sections and evaluates the impact of long cable systems on overvoltage characteristics. In Section 5, the focus is laid on schemes consisting of mixed OHL-cable sections. Finally, a conclusion is given in Section 6.

2. System description and modelling

A schematic of the considered SMP configuration is depicted in Fig. 1. Basic system parameters such as transmission capacity, rated dc voltage and submodule design are stated in Table 1.

Converter equipment as well as cable terminations are protected by surge arresters (SA). As the investigated types of overvoltages are in the range of temporary and slow-front overvoltages according to the classification in [15], the switching impulse characteristic of the SAs is considered as an adequate representation. The voltage-current characteristic of the cable arresters can be found in Appendix A. In the underlying station design, converter arm inductances are located on the dc side between submodule stacks and cable terminations. An overview

* Corresponding author.

E-mail addresses: max.goertz@kit.edu (M. Goertz), s.beckler@transnetbw.de (S. Beckler).

<https://doi.org/10.1016/j.epsr.2020.106603>

Received 11 February 2020; Received in revised form 21 June 2020; Accepted 29 July 2020

Available online 10 August 2020

0378-7796/ © 2020 The Authors. Published by Elsevier B.V. This is an open access article under the CC BY-NC-ND license (<http://creativecommons.org/licenses/by-nc-nd/4.0/>).

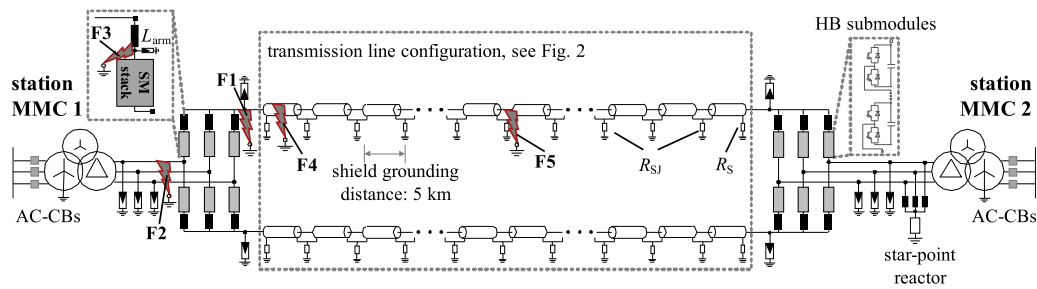


Fig. 1. Schematic of symmetrical monopolar configuration.

Table 1
Selected parameters of symmetrical monopolar configuration.

Parameter	Value
rated power P_r	1 GW
nominal dc voltage (pole-to-ground) U_0	± 320 kV
nominal ac voltage (valve / grid side)	330 kV / 400 kV
line frequency f	50 Hz
short circuit level ac grid	45 GVA
X/R ratio ac grid	10
transformer configuration	wye-delta
number of submodules per arm N	256
average arm sum voltage	640 kV
average submodule voltage	2.5 kV
submodule capacitor C_S (absolute)	8.5 mF
submodule capacitor C_S (relative)	39 kJ/MVA
arm inductance L_{arm}	50 mH
clearing time ac circuit breakers T_C	80 ms
switching impulse protective level of arresters	1.7 p.u. @ 3 kA

of the investigated transmission system configurations is depicted in Fig. 2. Relevant design parameters of the cable and the OHL are stated in Appendix B. In order to evaluate the impact of very long land cable systems, two different transmission system configurations comprising either 200 km or 700 km onshore cable with extruded insulation are analysed. Then, case study results are extended to a scheme comprising mixed OHL and cable sections with a total length of 700 km. Along the cable system, a solid cable shield grounding is assumed every 5 km taking into account a grounding resistance of $R_{SJ} = 5 \Omega$ and $R_S = 0.1 \Omega$ at transition joints and cable terminations, respectively. Cable and OHL sections are modelled by frequency-dependent line models in

accordance with the theory given in [16]. The submodule stacks of the MMCs are represented through a Type 4 detailed equivalent circuit model according to the classification given in [17]. Time-domain simulations are carried out using PSCAD/EMTDC. For the parametric study a solution time step of $5 \mu s$ is considered. In assessing voltage reversals during a cable fault in the vicinity of the converter station, a reduced solution time step of $0.5 \mu s$ is used.

2.1. Control and protection

Station 1 operates in an active/reactive power control mode and station 2 acts as a dc voltage/reactive power controlled station. The protection system of each converter station consists of valve over-current, submodule under-/overvoltage, dc pole-to-ground under-/overvoltage as well as a dc pole-to-ground voltage unbalance criterion. The protection functions comprise artificial delays in order to address delays due to data acquisition and processing, as further described in [13]. After protection tripping, all IGBTs of the affected converter are blocked and an opening order is sent to the ac circuit breakers (AC-CBs). Protection thresholds and controller parameters are held constant for all investigated transmission system configurations.

2.2. Parametric study framework

During the lifetime of an HVDC system, the cable system might experience different fault types such as station internal faults or cable faults, as indicated by HVDC failure statistics summarized in [18]. Therefore, a reliable insulation co-ordination strategy of the cable system requires an evaluation of a broad range of various fault types and locations. The considered fault types and converter operation

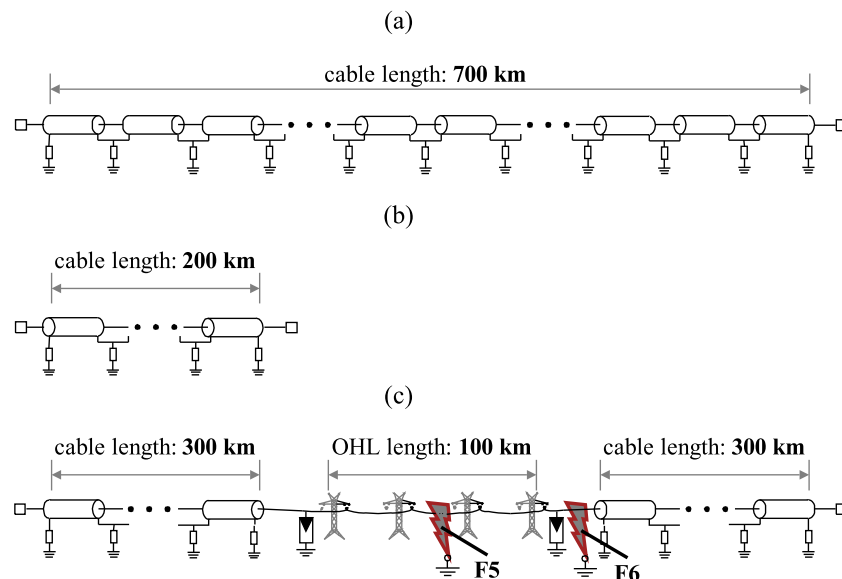


Fig. 2. Single pole diagram of investigated transmission system configurations: (a) 700 km cable, (b) 200 km cable and (c) 700 km OHL-cable mixed system.

Table 2
Parametric study framework.

Description	Configuration
1. power set point at station 1	a) $+P_r$ (ac in-feed, inverter mode of station 1), $+Q_r$ (cap.) b) $-P_r$ (ac export, rectifier mode of station 1), $+Q_r$ (cap.) c) 0 GW (zero load), $+Q_r$ (cap.)
2. fault type	F1: positive dc pole-to-ground fault at cable termination of station 1 F2: phase α -to-ground fault at transformer valve side of station 1 F3: positive arm $p1$ -to-ground fault at station 1 F4: cable core-to-screen-to-ground fault at 1 km distance from station 1 (positive dc pole) F5: cable core-to-screen-to-ground fault at 50 % of scheme length (positive dc pole) F6: positive dc pole-to-ground fault at cable termination located at the OHL-cable transition station (only in case of mixed systems)
3. fault resistance	0.1 Ω , 10 Ω
4. fault synchronisation	a) zero crossing of phase α -to-ground voltage at transformer valve side b) zero crossing of ac current in phase α at transformer valve side
5. fault instant	a) $\omega \cdot t = 0^\circ$, b) $\omega \cdot t = 45^\circ$ c) $\omega \cdot t = 90^\circ$, d) $\omega \cdot t = 225^\circ$ e) $\omega \cdot t = 270^\circ$ after zero crossing

modes are stated in Table 2. Due to the identical design of both converter stations and due to the consideration of different converter operation modes it is sufficient to investigate station internal faults only at station MMC 1. In order to ensure that the determined voltage transients reflect worst case conditions, different pre-fault converter operation modes and various fault instants are taken into account. The reactive power set point at both stations is set to the rated reactive power in order to ensure highest ac voltages at transformer grid side during normal operation.

3. Systematic approach to evaluate overvoltages

In order to assess the voltage stresses affecting the HVDC cable system, a systematic approach for determining overvoltage parameters is developed. First, a broad range of parametric variations are performed by means of EMT-software. Then, obtained data is systematically evaluated during post-processing by numerical computing software. Along the cable system, voltage measuring points are placed in equidistant sections with a length of 5 percent of total scheme length. For each run of the parametric study all voltage measuring points along the cable sections of both dc poles are taken into consideration for post-processing. This measure allows to characterise the voltage stresses at each point along the cable.

Besides the highest occurring crest value of the voltage at each measuring point along the cable, further parameters are used to specify the voltage stresses. The time-to-peak is used to describe the front of the overvoltage. Here, the time-to-peak value T_p is defined as the time interval between $\pm 5\%$ deviation of rated dc voltage U_0 and the point in time of the highest peak value. It should be mentioned that this definition is not in line with the time to crest defined in [19] for impulse voltage tests, as further discussed in Section 4.5. The front of the overvoltage may consist of superimposed voltage oscillations, as shown in Fig. 3 for exemplary overvoltage shapes. In particular for mixed schemes, the evaluation of time-to-peak values can be misleading because there are wave shapes which are characterised by a long front time but a high voltage gradient. Therefore, absolute maximum voltage gradients are considered as additional parameter to describe the front of the overvoltage. In order to avoid that numerical oscillations might distort the obtained gradient, an average voltage gradient along five solution time steps is calculated. In order to facilitate a profound analysis, the aforementioned parameters such as peak value, time-to-peak and maximum voltage gradient are determined at each voltage measuring point along the cable for all investigated parameter combinations.

4. Impact of very long cable systems

This section focuses on schemes comprising solely cable sections and performs a comparison between the cable lengths of 200 km and 700 km. Based on presented case study results, the impact of long cable systems on voltage stresses is discussed. Occurring voltage stresses are classified in overvoltages with same polarity as the dc operating voltage and in overvoltages with opposite polarity to the dc operating voltage. An overvoltage with opposite polarity to the dc operating voltage might occur at the faulty dc pole during the cable discharge process. In the following, such voltage shapes are defined as voltage reversals.

4.1. Highest voltage peak values along the cable system

For each run of the parametric study the highest peak values of all measured voltages along the cable systems of both dc poles are determined during post-processing. A peak value describes the highest occurring crest value of either an overvoltage with same polarity as the dc operating voltage or of a voltage reversal. In the next step, the highest voltage peak values of all runs of the parametric study related to the same fault type and the same converter operation mode are identified. Results are depicted in Fig. 4 (a)-(b) in per unit (p.u.) of rated dc voltage U_0 . All investigated dc side faults (F1, F3, F4, F5) are located along the positive dc pole. Therefore, voltage reversals occur at the positive dc pole for the faults F1 and F3-F5. An overvoltage with same polarity as the dc operating voltage can be observed at the negative dc pole for all investigated fault types. It should be noted that a single phase-to-ground fault at transformer valve side (F2) leads to an overvoltage with same polarity as the dc operating voltage at both dc pole conductors. For both considered cable lengths, highest peak values of the overvoltages occur during a cable fault at 50 % cable length (F5) at zero load operation (0 GW). Absolute maximum overvoltage levels are 1.76 p.u. and 1.72 p.u. for cable lengths of 200 km and 700 km, respectively. Moreover, it is noticeable that the overvoltage peak levels reach higher values in the 200 km system than in the 700 km system for all investigated fault types. The highest peak value of all voltage reversals is caused by a cable fault in the vicinity of the converter station (F4). The highest peak value of all voltage reversals stays below 1 p.u. and is not affected by the total scheme length.

4.2. Voltage profiles along the cable system

A worst-case voltage profile along the cable is shown in Fig. 5 (a)-(b) for each fault type. Within this study, a worst-case is defined as the

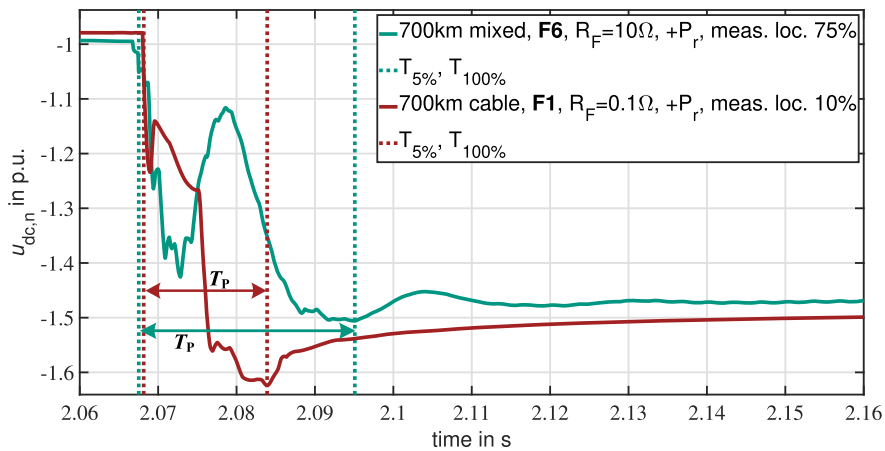


Fig. 3. Definition of the time-to-peak for different overvoltage wave shapes.

highest peak value of the voltage at each measuring point along the cable of all parameter variations related to the same fault type. Hence, a voltage profile of the same fault type might consist of different simulation runs. Fig. 5 (a) contains the voltage profiles in case of overvoltages with same polarity as the operating voltage and Fig. 5 (b) shows the voltage profiles during voltage reversals. As can be seen, highest overvoltage peaks occur in the middle of the cable route of the healthy dc pole during F5. This finding is also achieved in [5] and further discussed in Section 4.3.1. It is worth emphasising that an analysis of several voltage measurements along the cable route is of utmost importance as highest overvoltages occur inside the cable and

not at the converter stations. With regard to voltage reversals caused by the cable discharge process, highest peak values occur at the cable termination adjacent to the faulty cable section in case of a cable fault in the vicinity of the converter station (F4). As shown in [4,20], the voltage reversals at the faulty cable are caused by the intrinsic discharge process of the cable through the fault impedance, see Section 4.3.2.

4.3. Build-Up of the voltage shapes leading to highest crest values

This section describes the voltage build-up along the cable for the

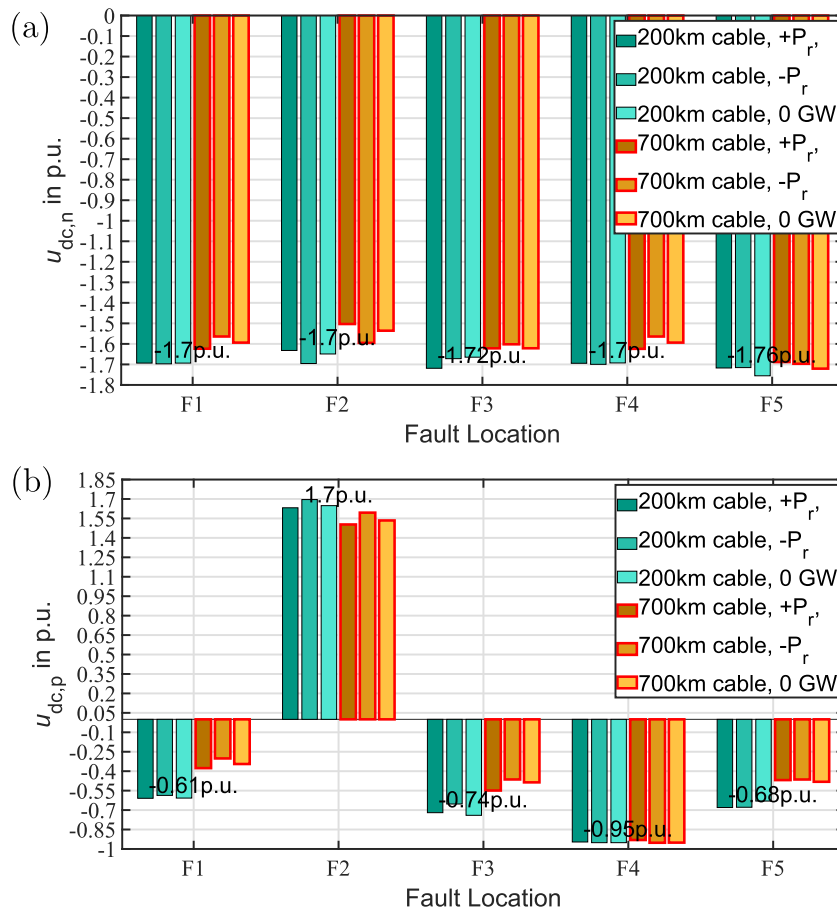


Fig. 4. Highest peak values of all measured voltages along the cable system for each fault type F1 - F5, power set point and cable length: (a) measured voltages along negative dc pole, (b) measured voltages along positive dc pole.

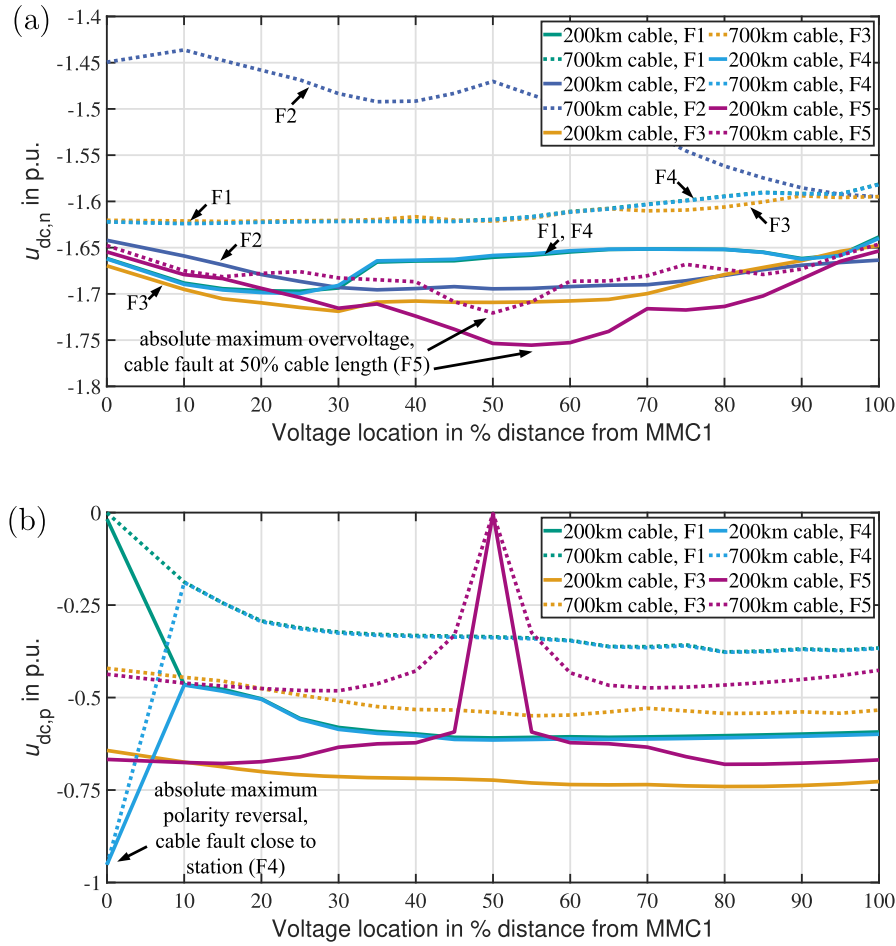


Fig. 5. Worst case voltage profiles along the cable system for different fault types F1 - F5 and cable lengths: (a) negative dc pole, (b) positive dc pole.

fault type and parameter combination that leads to the highest peak values of the voltage. Section 4.3.1 focuses on the worst case overvoltage with same polarity as the dc operating voltage and Section 4.3.2 focuses on the worst case voltage reversal.

4.3.1. Overvoltage during cable fault F5

As described in Section 4.1, the highest overvoltage peak with same polarity as the dc operating voltage is caused by a cable fault at 50 % of scheme length (F5) at zero/low load operation of the converters. Fig. 6 presents the cable core-to-ground voltage $u_{dc,n}$ at different voltage measuring points along the cable for both considered system lengths during the worst-case run of F5. As can be seen in the zoomed part of Fig. 6 (b), both converters block their IGBTs at the same time instant (green curve).

For the 200 km system, blocking instants of both converters are slightly different. As the cable fault occurs at 50 % of scheme length, the travelling waves triggered by the fault reach both converter stations at the same time instant. At zero/low load operation and with an equal reactive power set point at both converter stations, the protection thresholds are violated at both stations at nearly the same time instant. Therefore, the blocking instants of both converter stations are nearly identical. At the instant of IGBT blocking t_{by} , the voltage $u_{dc,n}$ at the respective converter station $y \in \{1, 2\}$ consists of an impulse voltage u_{fy} superimposed on dc operating voltage, as shown in the zoomed part of Fig. 6. The impulse voltages u_{f1} and u_{f2} represent forward travelling waves that propagate from both converter stations into the cable. This process is visualized in the simplified lattice diagram shown in Fig. 7.

Here, Z_c is the surge impedance of the cable and τ is the propagation time along the cable with length l . In case both converters are blocked

at the same time instant t_{b1} , a first superposition of u_{f1} and u_{f2} occurs in the middle of the cable route at $t_m = t_{b1} + \tau/2$. Otherwise, the location of the first superposition might deviate from the center of the cable route. In case of the same blocking instant of both converters, the voltage at the point of superposition $x_m = l/2$ can be written as the sum of both travelling waves superimposed on the dc operating voltage:

$$u(x_m, t_m) = U_0 + u_{f1} \cdot e^{-\alpha x_1} + u_{f2} \cdot e^{-\alpha x_2}. \quad (1)$$

The exponential parts in (1) describe the attenuation of the travelling wave along the cable distance x_y . For simplicity, dispersion effects are neglected in (1) and α is assumed to be a constant. In fact, it is obvious that the attenuation constant α is frequency-dependent. For the considered cable design α is approximately $\alpha(10 \text{ Hz} \dots 1 \text{ kHz}) \approx 0.36 \times 10^{-3} \frac{1}{\text{km}} \dots 1.6 \times 10^{-3} \frac{1}{\text{km}}$. Applying (1), the superposition of both travelling waves can be estimated based on the assumption that α is a constant. In the 200 km system, the highest overvoltage peak along the cable is caused by the first superposition of u_{f1} and u_{f2} . In the 700 km system, the superposition of u_{f1} and u_{f2} results in a first peak value during the front of the overvoltage, but not the highest peak voltage, as can be seen Fig. 6 (b). Instead, in the 700 km system the highest peak voltage occurs at $t = t_{b1} + (3 \cdot \tau)/2$ after the first reflection of the impulse voltages at the opposite station, as indicated in Fig. 7. Here, r_{cy} represents the voltage reflection coefficient at the blocked converter station. In the 200 km system, the impulse voltage reflected at the opposite station at $t = t_{b1} + \tau$ is limited by the surge arresters. The lower peak values of the overvoltages in the 700 km system compared to the 200 km system can be explained by the following reasons: i) for very long cable systems the cable self attenuation effect dampens the impulse voltages propagating along the cable, ii) the

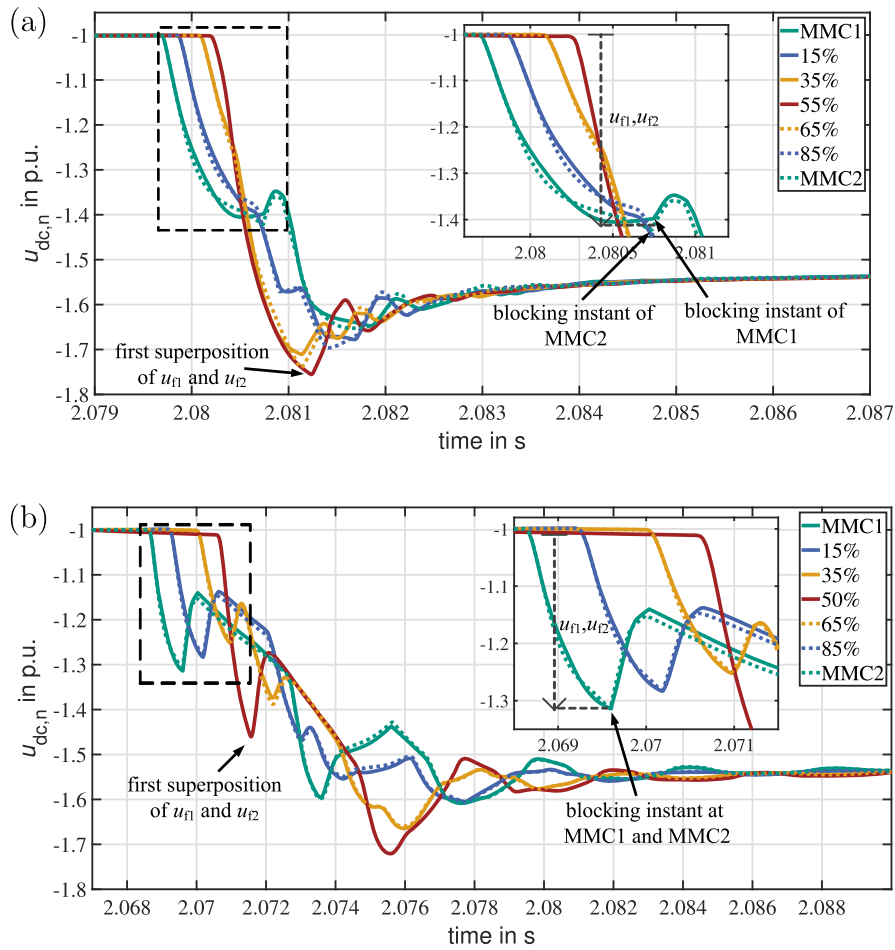


Fig. 6. Overvoltage build-up along the cable of the negative dc pole during a cable fault at the positive pole (F5): (a) cable length 200 km, (b) cable length 700 km.

initial impulse voltage at the converter stations u_{fy} as well as the voltage gradient prior to IGBT blocking decreases for very long cable sections. Besides, it is worth mentioning that the transient system behaviour is affected by considered protection thresholds and blocking delays as well as converter control prior to blocking.

4.3.2. Voltage reversals during cable fault F4

The highest peak of all voltage reversals occurs at the cable termination during a cable fault in the vicinity of the converter station (F4).

The pole-to-ground voltage measured at the cable termination of the positive dc pole is depicted in Fig. 8 for such an event.

As the voltage reversals at the faulty cable section are independent of the total scheme length, results are shown only for a scheme length of 200 km. The voltage build-up along the faulty cable section during F4 can be explained based on the simplified lattice diagram shown in Fig. 9. The fault F4 with the fault resistance R_f occurs at $t = t_f$ and provokes an impulse voltage with opposite polarity to the dc operating voltage. This travelling wave propagates towards the converter station.

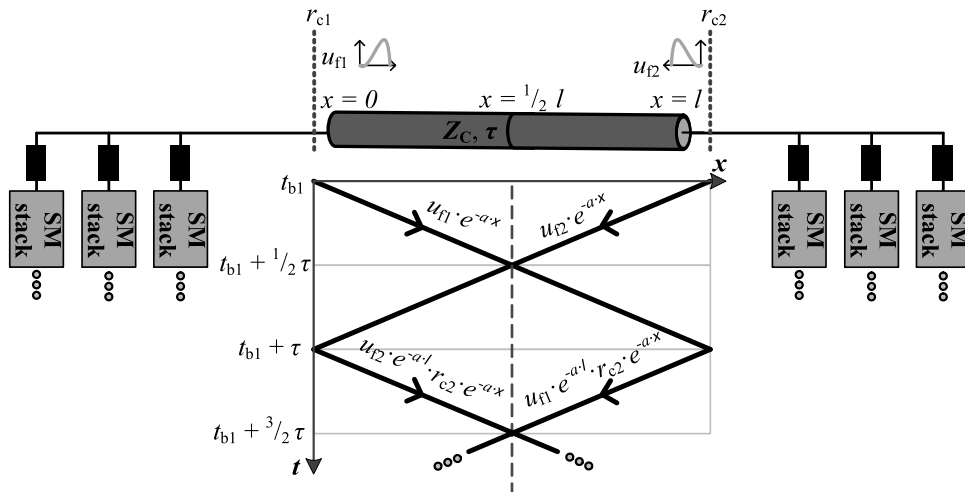


Fig. 7. Lattice diagram along the cable of the negative dc pole during a cable fault at the positive pole (F5).

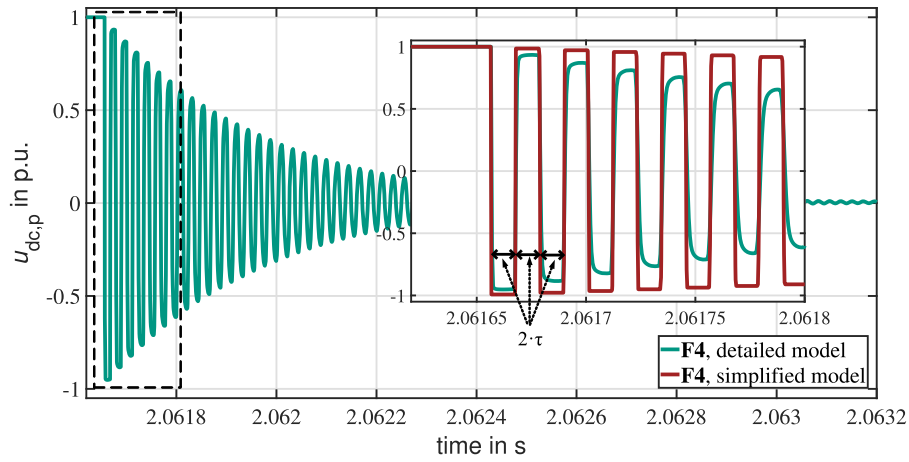


Fig. 8. Voltage reversals measured at the cable termination located at converter station MMC1 during cable fault F4. Considered cable length: 200 km.

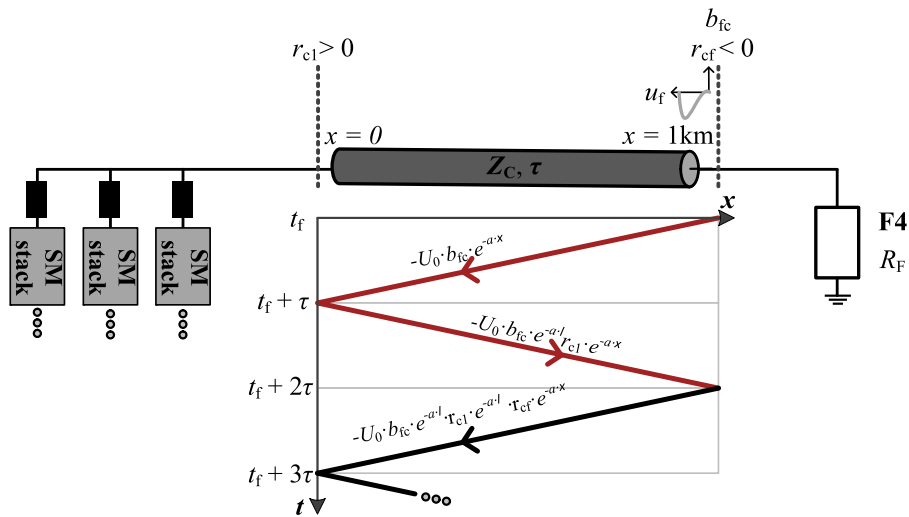


Fig. 9. Lattice diagram of the cable section between F4 and station MMC 1. Cable of the positive dc pole during a cable fault at the positive dc pole (F4). Red line: impulse with opposite polarity to the operating voltage, black line: impulse with same polarity as the operating voltage.

The magnitude of the forward propagating impulse voltage depends on the ratio of the cable's surge impedance and the sum of surge impedance and fault resistance $b_{fc} = Z_c / (Z_c + R_F)$. The voltage reflection coefficient at the discontinuity between cable and the unblocked converter r_{cl} is positive and close to 1 due to the high impedance of the arm reactors for fast front transients compared to the surge impedance of the cable. Therefore, the backward travelling wave is with same polarity as the incoming wave at the cable termination. The fault represents a discontinuity between the surge impedance of the cable and the fault impedance. The voltage reflection coefficient r_{cf} is less than zero at the fault location. Therefore, the reflected travelling wave is of opposite polarity to the incoming wave at $t = t_f + 2\tau$. For a better visualization of the travelling wave effects, the zoomed part of Fig. 8 contains a comparison of a frequency dependent cable model (green curve) and a simplified cable model (red curve). The simplified model uses the Bergeron model and represents the cable through a lossless line characterized by its surge impedance and travel time. As clearly depicted, the voltage at the cable termination changes its polarity every 2τ . For the considered system the theoretical peak of the voltage reversal is 1 p.u. For cable faults in the vicinity of the converter station, the propagation time of the travelling wave between the fault location and the converter station is in the range of several microseconds. In such cases, the discharge process of the faulty cable section through the fault impedance occurs in the range of several hundreds of microseconds. For control and protection purposes, HVDC converter stations

are equipped with voltage dividers and instrument transformers. The commonly used measuring equipment is characterized by a certain bandwidth and requires a certain processing delay [21]. Due to the short time interval between the voltage reversals, the peak value of the voltage reversal is reached before the protection system of the converter station has tripped. Therefore, the control and protection strategy of the converter only has a minor impact on the voltage reversals during F4. Instead, the discharge process is mainly affected by the propagation constant of the cable and the assumed fault impedance. For the sake of completeness, it should be mentioned that the voltage reversals during the cable fault F4 occur not only in symmetrical monopolar scheme configuration. The cable discharge during F4 is independent of the selected HVDC scheme configuration, as shown in [13].

4.4. Representative overvoltages

The overvoltage shapes measured at the location of the highest peak value are depicted in Fig. 10 for a fault at 50 % of scheme length (F5) and for a phase-to-ground fault at transformer valve side (F2).

The overvoltage wave shape provoked by F5 consists of a voltage increase up to a peak value followed by a temporary overvoltage (TOV) at a decreased voltage level. The front parameters of the overvoltage such as rise time, voltage gradient and peak value are strongly affected by the cable length. The TOV level of the overvoltage depends on the considered SA characteristic and equals approximately 1.5 p.u. for both

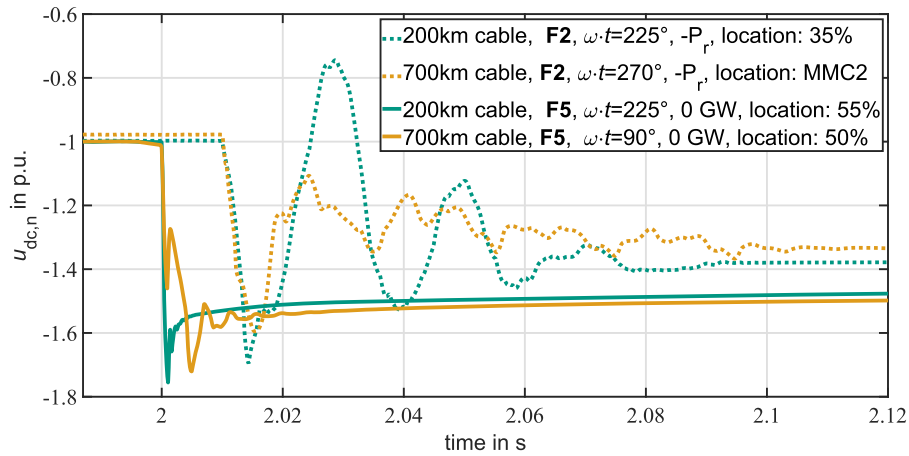


Fig. 10. Overvoltage shapes leading to the highest peak values during F2 and F5 for the considered cable lengths of 200 km and 700 km.

cable lengths. The TOV persists until the cable is discharged through intrinsic shunt or stray impedances to ground or auxiliary earthing breakers are applied, see [4] for further explanation. During F2, voltage oscillations can be observed at the cable system until the AC-CBs have cleared the fault. The amplitude of the voltage oscillation increases for shorter cable lengths.

4.5. Overvoltage characteristics

This section focuses on overvoltages with same polarity as the dc operating voltage and determines additional characteristics during the front of the overvoltage. Fastest time-to-peak values and steepest voltage gradients of all overvoltages measured along the cable route of the

healthy dc pole under consideration of all parameter variations are depicted in Fig. 11 (a)-(b). It should be noted that Fig. 11 (b) contains the steepest gradients that occur during the front of the overvoltages and not the mean gradients. In the 200 km system, fastest time-to-peak values T_p are in the range of 700 μ s and occur during a fault at the cable termination (F1). In the 700 km system, fastest time-to-peak values are in the range of several milliseconds. According to the classification given in the relevant standards for insulations co-ordination [22,23], the determined front times are in the range of slow-front overvoltages and temporary overvoltages. For external insulation, the severity of slow-front overvoltages is usually associated with the front-time of the wave shape [24]. For dc cables with extruded insulation, the impact of the time-to-peak value on the breakdown or ageing process of

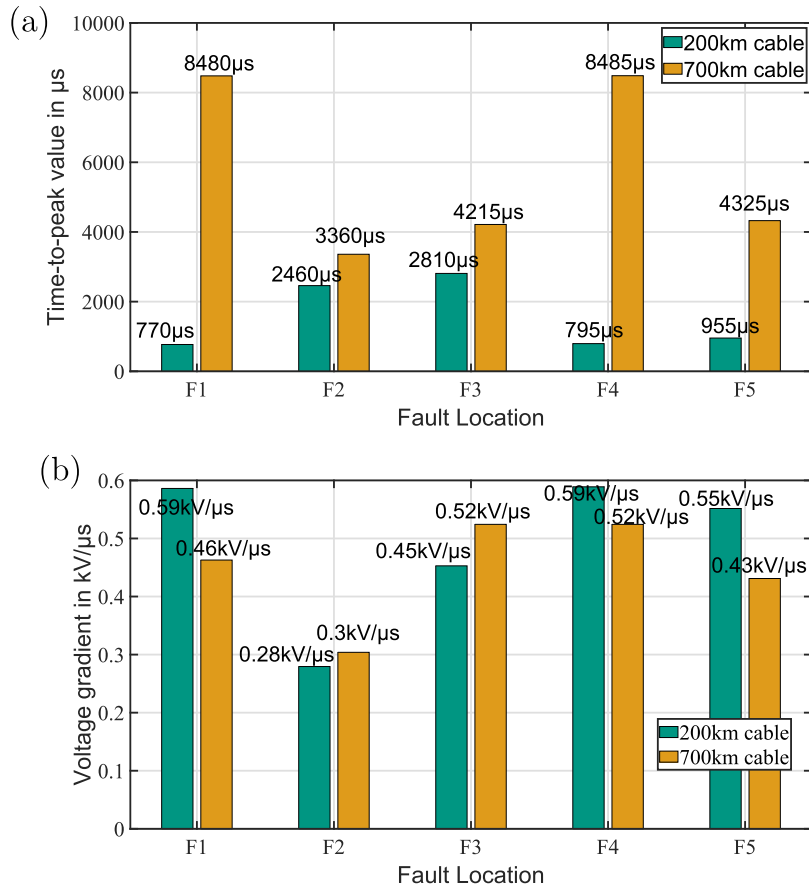


Fig. 11. Impact of cable length on overvoltage front parameter: (a) fastest time-to-peak values, (b) absolute maximum voltage gradients.

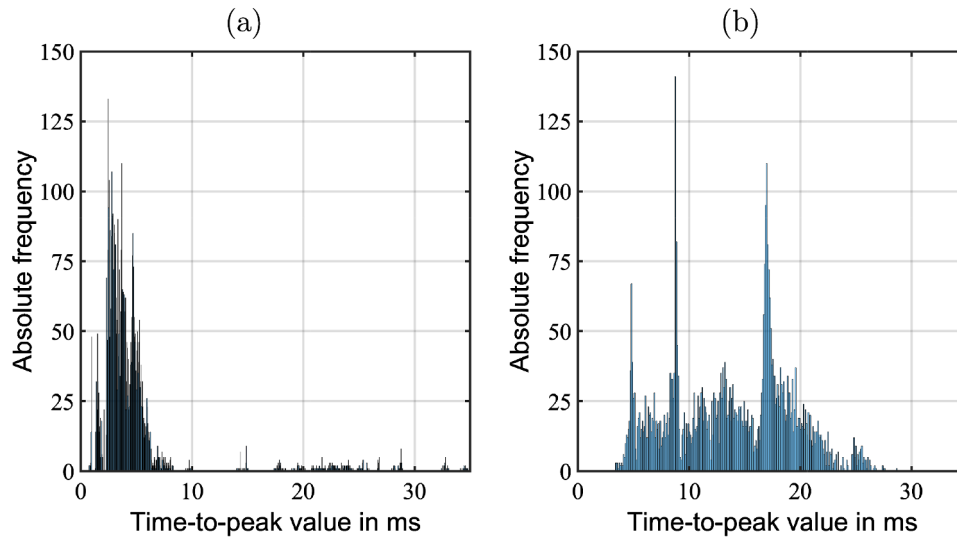


Fig. 12. Histogram of all determined time-to-peak values under consideration of all voltage measuring points along the cable route: (a) cable length 200 km, (b) cable length 700 km.

the polymeric insulation is not yet fully established and merits more investigation. This issue is part of the currently ongoing discussions on HVDC cable systems exposed to non-standard voltage wave shapes [1]. It is important to clarify that the fastest front times do not occur at the same spatial location as the highest peak values of the overvoltages and also not for the same parameter combination. A combination of the highest peak value of the overvoltage and the fastest rise time for the impulse voltage tests might result in unrealistic voltage stresses in the cable insulation. It can be observed that the voltage gradients during the front of the overvoltage take on smaller values with increasing cable length. Fig. 12 shows a histogram of all determined time-to-peak values.

For long cable systems, a wider range of time-to-peak values exists. The fastest front times occur only for certain parameter combinations. One could therefore assume that the fastest front times are characterised by a lower probability of occurrence. Nonetheless, it is important to emphasize that statements regarding the probability of occurrence shall be treated with utmost caution since the distribution of the time-to-peak values depends on the considered parametric framework. It should be noted that a phase-to-ground fault at transformer valve side (F2) might evoke an overvoltage on the dc side where the peak value is reached only after several half-cycles of ac voltage. Therefore, certain T_p values are in the range of 20 ms to 30 ms for both system lengths.

5. Impact of schemes comprising mixed OHL-Cable sections

This section evaluates the voltage stresses along the cable route for HVDC schemes comprising mixed OHL-cable sections. The first part of this section focuses on long cable sections in combination with an OHL, while the second part unveils the voltage stresses in case of short cable sections in combination with OHLs.

5.1. Long cable section in combination with OHL

The considered scheme length is 700 km. As introduced in Fig. 2, the mixed transmission scheme comprises an overhead transmission line with a length of 100 km embedded between two cable sections, each with a length of 300 km. Occurring cable voltage stresses are compared between the mixed transmission system and the scheme comprising solely cable sections. The worst case voltage profiles under consideration of all investigated fault types are depicted in Fig. 13 (a)-(b). As previously introduced, Fig. 13 (a) shows the voltage profiles in

case of overvoltages with same polarity as the operating voltage and Fig. 13 (b) presents the voltage profiles during voltage reversals. The vertical black lines represent the locations of the transition stations between cable route and OHL.

As can be seen in Fig. 13 (a), cable overvoltages reach similar peak values in both transmission systems. However, the spatial dependency of the voltage profiles along the cable route is more pronounced for the mixed transmission system. The transition stations represent a discontinuity between the surge impedance of the cable and the surge impedance of the OHL. Therefore, additional travelling wave reflections occur along both cable sections within a shorter period of time. In the mixed system the highest occurring peak value of all overvoltages is provoked by a station internal arm-to-ground fault (F3), as depicted in Fig. 14. With regard to voltage reversals, the highest peak value is caused by the fault F4 in both schemes. The highest peak value of all voltage reversals remains below 1 p.u. in the considered mixed OHL-cable system. The fastest time-to-peak values and the steepest voltage gradients of all cable overvoltages with same polarity as the dc operating voltage are summarized in Fig. 15. For the mixed transmission system, additional fault types have to be taken into consideration. It can be observed that faults at the transition station (F6) lead to the shortest front times and the steepest voltage gradients compared to all fault types investigated. Therefore, the cable system might experience faster time-to-peak values and significant steeper voltage gradients in case of a mixed transmission system.

5.2. Short cable section in combination with OHL

The previous section focused on a mixed transmission scheme comprising long cable sections. However, it is to be expected that more severe voltage stresses may occur with short cable lengths, since travelling wave effects are more pronounced in case of shorter cable sections. Therefore, this section is intended to outline the effects of a cable fault on the voltage reversals occurring in case of a transmission scheme with a short cable section. The considered transmission system consists of a cable - OHL - cable configuration. A short cable with a length of 1 km is embedded between a converter station and an OHL section. The OHL with a length of $l_{OHL} = 15$ km is connected to a long cable. The cable fault occurs in the vicinity of transition station 2 in a distance of $l_{C2} = 10$ km. Fig. 16 shows a simplified lattice diagram for such a fault type.

For reasons of clarity, the lattice diagram does not take into account the attenuation effects of the travelling waves. The cable fault provokes

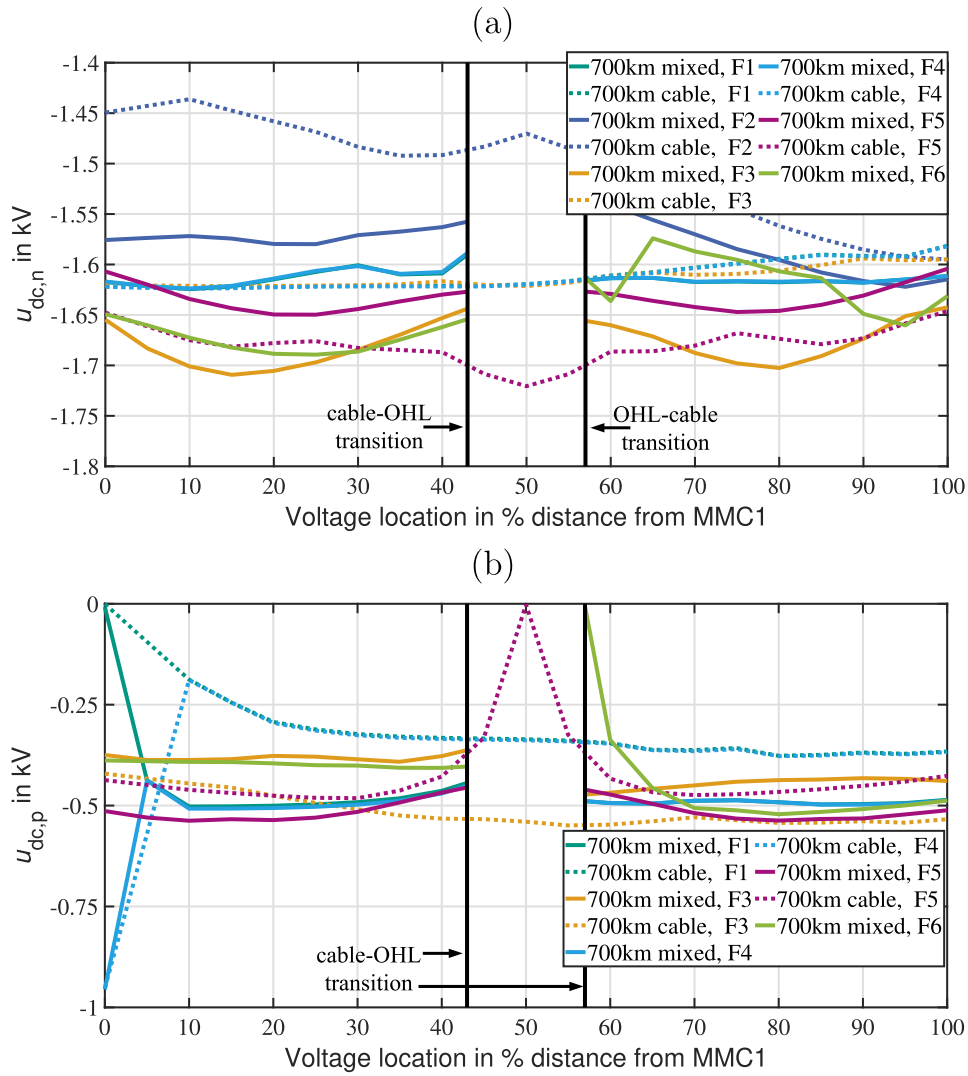


Fig. 13. Worst case voltage profiles along the cable system as a function of fault type F1 - F6 and transmission line configuration. Considered system length 700 km: (a) negative dc pole, (b) positive dc pole.

an impulse voltage with opposite polarity to the operating voltage. The peak value of the forward travelling wave is $U_0 \cdot b_{fc}$ with $b_{fc} = Z_C / (Z_C + R_F)$. The travelling wave propagates towards transition station 2. At transition station 2, the travelling wave is partially

transmitted into the OHL. Along the OHL, the peak value of the forward propagating wave is $U_0 \cdot b_{fc} \cdot k_{cohl}$ with $k_{cohl} = (2 \cdot Z_{OHL}) / (Z_C + Z_{OHL})$. Note that $k_{cohl} > 1$ due to the higher surge impedance of the OHL compared to the surge impedance of the cable: $Z_{OHL} \gg Z_C$. At transition

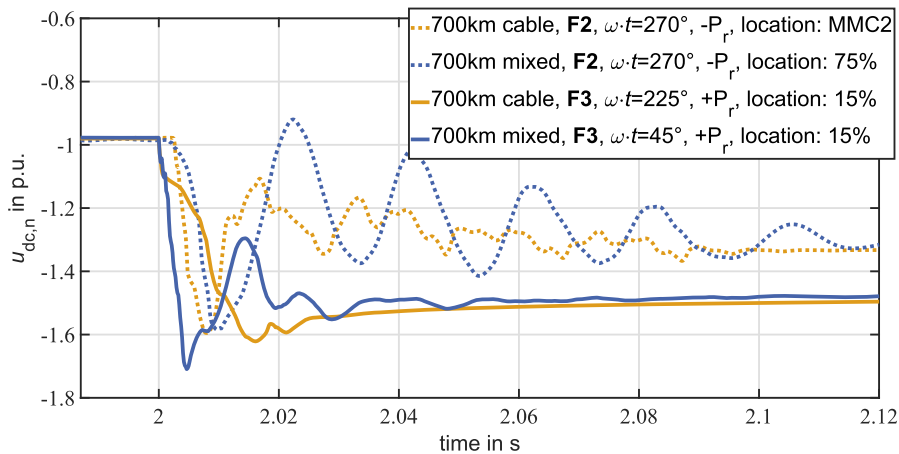


Fig. 14. Overvoltage shapes leading to the highest peak values for the faults F2 and F3, considered scheme length: 700 km. Comparison between a scheme comprising solely cable and a scheme comprising mixed OHL-cable sections.

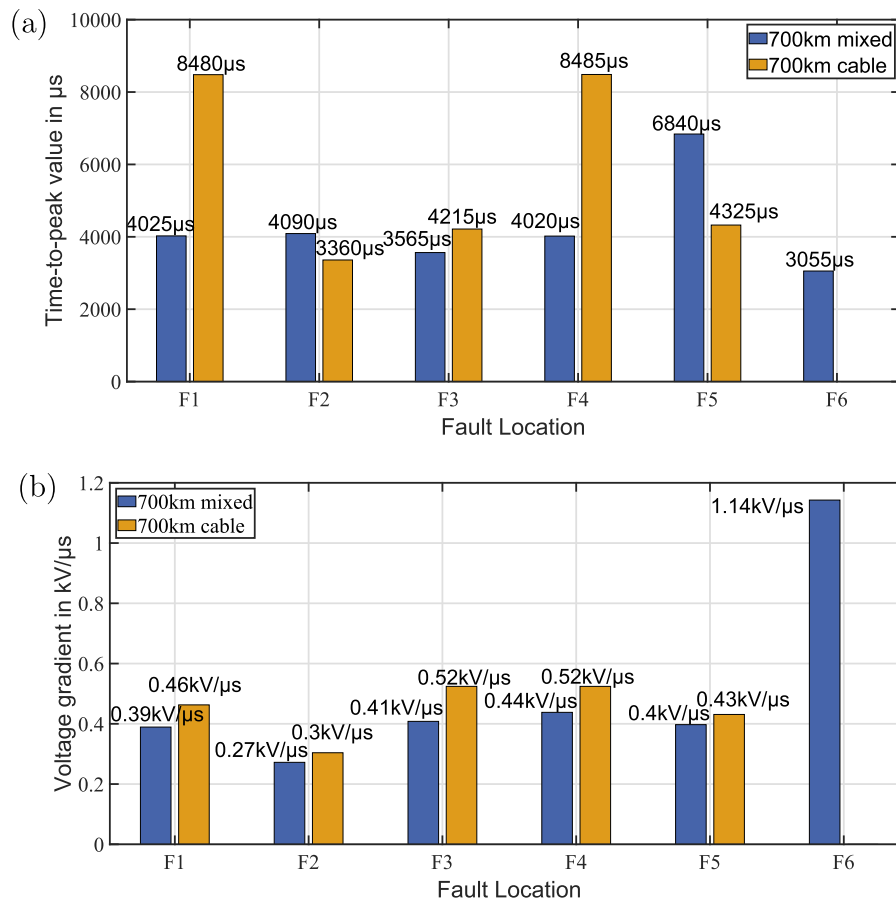


Fig. 15. Impact of transmission line configuration on the front parameters of the overvoltage wave shapes, considered system length 700 km: (a) fastest time-to-peak values, (b) absolute maximum voltage gradients.

station 1, parts of the forward travelling wave are transmitted into the cable. Along the short cable, the peak value of the forward propagating voltage wave is $U_0 \cdot b_{fc} \cdot k_{cohl} \cdot k_{ohl}$ with $k_{ohl} = (2 \cdot Z_C) / (Z_C + Z_{OHL})$. The voltage reflection coefficient at the converter station r_{c1} is positive due to the high impedance of the arm reactors for fast front transients, as mentioned in Section 4.3.2. In contrast to the cable fault F4 described in Section 4.3.2, the voltage reflection coefficient r_{cohl} at the discontinuity between the surge impedance of the short cable and the surge impedance of the OHL is also positive. Therefore, the backward travelling waves are with the same polarity as the forward travelling waves along the short cable section. This aspect leads within a short time to multiple superpositions of travelling waves with same polarity along the short cable section, as indicated by the red lines in the lattice diagram in Fig. 16. Due to the short propagation time τ_{c1} along the short cable compared to $(\tau_{OHL} + \tau_{c2})$, the multiple superpositions can cause a significant peak value of the voltage reversal along the cable section. The voltage reversals measured at the cable termination at station 1 are depicted in Fig. 17.

As clearly depicted, the peak value of the voltage reversals at the short cable is significantly higher than 1 p.u. The highest peak value of the voltage reversals occurs before the converter is blocked. The considered station design contains an optional dc reactor L_{dc} , as indicated in Fig. 16. An additional dc reactor might be installed in mixed transmission schemes. To address this project specific design parameter, the dc reactor L_{dc} is varied in the range of 0... 50 mH. An additional dc reactor or instead higher values of the arm reactors increase the voltage reflection coefficient at the cable termination. Therefore, higher peak values of the voltage reversals can be observed with increasing values of L_{dc} , as shown in Fig. 17. Finally, it should be noted that the presented scenario with a short cable section as well as the consideration of an

additional dc reactor represents an extreme assumption. Nonetheless, it is important to point out that the voltage stresses affecting the cable system are more severe for mixed transmission schemes comprising short cable sections. In particular with regard to short cable sections, special attention is required to ensure a reliable insulation co-ordination strategy. Therefore, a detailed project specific overvoltage analysis is essential for such systems. For the sake of completeness, it should be mentioned that mixed transmission schemes also require a special attention with regard to lightning overvoltages as the dc cable is exposed indirectly to lightning strokes in such systems. A comprehensive analysis of lightning overvoltages in mixed schemes with short cable sections can be found in [25,26].

6. Conclusion

In order to assess relevant overvoltage characteristics affecting HVDC cable systems in SMP configuration based on HB-MMC technology, a detailed parametric study has been carried out and a systematic approach to evaluate overvoltages is presented within this paper. The following list provides an overview of the main findings:

- A decrease of the overvoltage peak levels can be observed for very long cable route lengths. This statement is proven only for the considered cable route lengths of 200 km and 700 km.
- An increasing cable length leads to slower time-to-peak values and lower voltage gradients for cable overvoltages with same polarity as the dc operating voltage.
- Time-to-peak values have to be evaluated carefully as the front of the overvoltage might consist of superimposed voltage oscillations.
- In the considered systems, fastest time-to-peak values and highest

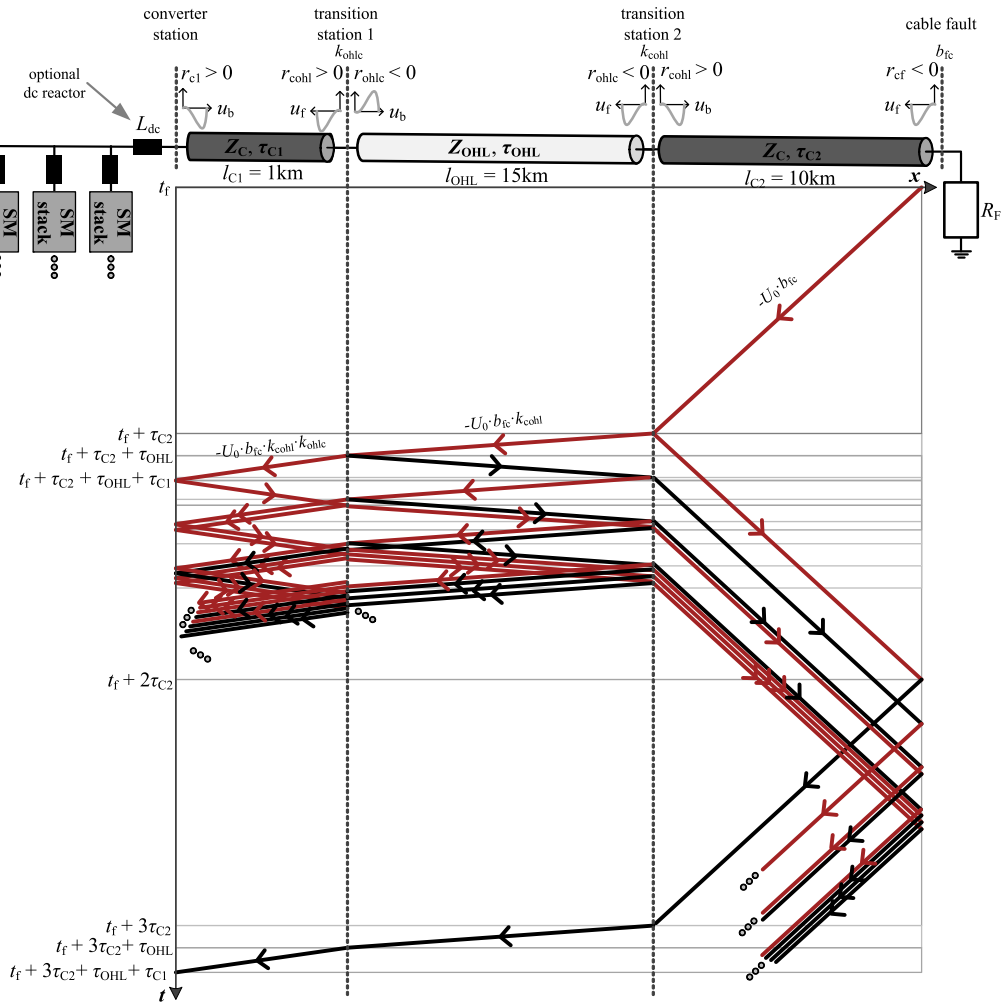


Fig. 16. Simplified lattice diagram for a cable - OHL - cable configuration in case of a cable fault at $l_{C2} = 10$ km. Red line: impulse with opposite polarity to the operating voltage, black line: impulse with same polarity as the operating voltage.

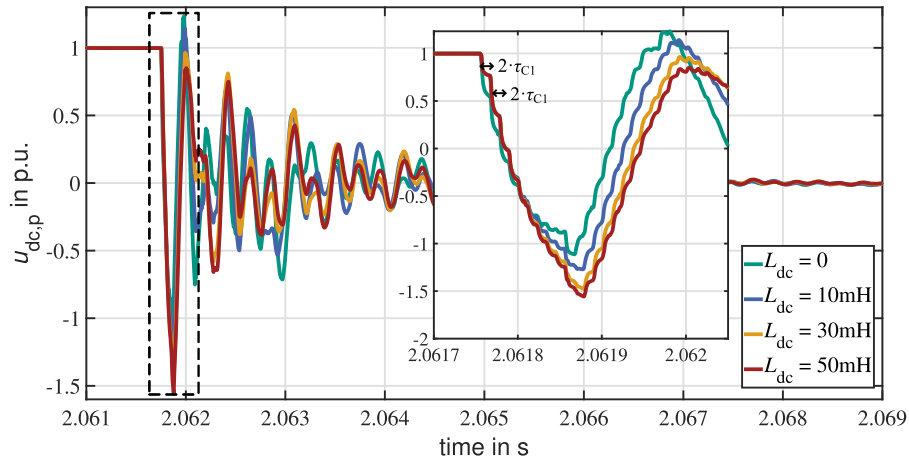


Fig. 17. Voltage reversals measured at the cable termination of a short cable section during a cable fault at $l_{C2} = 10$ km. The cable termination is located at the converter station.

peak values of the overvoltages occur not at the same measuring location and not for the same parameter combination. Therefore, a combination of the fastest time-to-peak value and the highest overvoltage peak for testing purposes might result in unrealistic cable stresses.

- In mixed OHL-cable systems, faster time-to-peak values and

significantly steeper voltages gradients occur compared to schemes comprising solely cable sections. For mixed system comprising long cable sections the peak values of the overvoltages are similar compared to schemes comprising solely cable sections.

- In case of mixed systems comprising a short cable section, multiple superpositions of travelling waves occur for certain fault types and

cause severe voltage reversals and overvoltages. Therefore, cable overvoltages in such schemes are difficult to predict, since the system behaviour depends strongly on the projects specific configuration.

For the sake of completeness, it should be mentioned that further project specific parameters such as converter station design or the transformer vector group might affect cable overvoltages, as outlined in [3,7]. Future research is required in order to examine if the determined parameters such as overvoltage level, front time and voltage gradient represent critical stresses for the cable insulation. It is worth mentioning that besides the presented overvoltage characteristics, other parameters such as duration of TOV appear relevant for the design of the cable system. The results provided within this paper represent a profound starting point for further work on insulation-coordination of HVDC cable systems and related high voltage testing issues. Therefore, obtained results are of importance with regard to upcoming cable projects in symmetrical monopolar HB MMC-HVDC configuration.

Appendix A. Surge arrester characteristic

The residual voltage of the cable arresters is 544 kV at a discharge current of 3 kA for a current impulse with a 30/60 μ s wave shape. The corresponding voltage-current characteristic of the cable arresters is stated in Tab. A.3. Frequency dependent effects of the voltage-current characteristic are not taken into account as the investigated overvoltage shapes are in the range of slow-front overvoltages. The voltage-current characteristic is approximated by piece-wise linear resistances. An additional inductance of 3.5 μ H representing the lead wire is connected in series to the arrester model.

Table A3
Voltage-current characteristic of the considered metal-oxide surge arresters.

Discharge current in kA	Voltage in kV
0.003	480
0.03	493
3	544
12	578
30	605

Appendix B. Cable and OHL geometry

B1. Cable design

A cable configuration feasible for land application is considered. The cable line consists of two cables, one for each dc pole. Each cable is composed of a copper conductor with a cross-section of 2500 mm², inner semiconductive layer, main insulation made of dc XLPE, outer semiconductive layer, metallic screen and outer sheath. The thickness of the main insulation is 20 mm. The metallic screen with a cross-section of 150 mm² is made of aluminium. The cables are laid in flat formation with a conductor spacing of 0.6 m.

B2. Overhead line design

The considered tower geometry is depicted in Fig. B.18. The overhead line design comprises two pole conductors and two overhead ground wires (OHGW). Each dc pole consists of a quad bundle conductor.

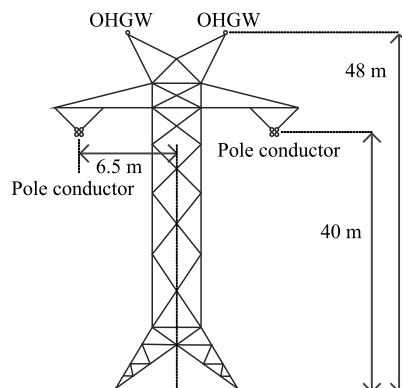


Fig. B18. Tower geometry.

CRediT authorship contribution statement

M. Goertz: Methodology, Software, Investigation, Writing - original draft, Writing - review & editing. **S. Wenig:** Conceptualization, Software, Writing - review & editing. **S. Beckler:** Resources, Conceptualization, Writing - review & editing. **C. Hirsching:** Visualization, Writing - review & editing. **M. Suriyah:** Validation, Writing - review & editing. **T. Leibfried:** Supervision, Writing - review & editing.

Declaration of Competing Interest

The authors declare that they have no known competing financial interests or personal relationships that could have appeared to influence the work reported in this paper.

References

- [1] M. Saltzer, Surge and extended overvoltages testing of HVDC cable systems, *Int. Conf. on Insulated Power Cables (Jicable'17)* (2017). Dunkerque, France, Nov.
- [2] F.B. Ajaei, R. Iravani, Cable surge arrester operation due to transient overvoltages under DC-Side faults in the MMC-HVDC link, *IEEE Trans. Power Del.* 31 (3) (2016) 1213–1222, <https://doi.org/10.1109/TPWRD.2015.2477493>.
- [3] H. Saad, P. Rault, S. Denetière, Study on transient overvoltages in the converter station of HVDC-MMC links, *Int. Conf. on Power System Transients (IPST'17)* (IPST17-185) (Seoul, Republic of Korea, June 2017).
- [4] S. Denetière, H. Saad, A. Naud, P. Honda, Transients on DC cables connected to VSC converters, *Int. Conf. on Insulated Power Cables (Jicable'15)*, (2015). Versailles, France, June
- [5] S. Mukherjee, M. Saltzer, Y.-J. Häfner, S. Nyberg, Cable Overvoltages for MMC based VSC HVDC Systems: Interactions with Converters, *Int. Colloquium on H.V. Insulated Cables, CIGRE Study Committee B1*, (2017). New Delhi, India, Oct
- [6] M. Goertz, C. Hirsching, S. Wenig, K.M. Schäfer, S. Beckler, J. Reisbeck, M. Kahl, M. Suriyah, T. Leibfried, Analysis of overvoltage levels in the rigid bipolar MMC-HVDC configuration (2019) 1–6. 10.1049/cp.2019.0025.
- [7] M. Greve, M. Koochack Zadeh, T. Rendel, A. Menze, Behaviour of the HVDC links with MMC technology during DC cable faults, *CIGRE Winnipeg 2017 Colloquium, Study Committees A3, B4 & D1*, Winnipeg, Canada, Sept. 2017, (2017). Winnipeg, Canada, Sept.
- [8] C. Freye, S. Wenig, M. Goertz, T. Leibfried, F. Jenau, Transient voltage stresses in MMC-HVDC links - impulse analysis and novel proposals for synthetic laboratory generation, *IET High Voltage* 3 (2) (2018) 115–125.
- [9] T. Karmokar, M. Saltzer, S. Nyberg, S. Mukherjee, P. Lundberg, Evaluation of 320kV extruded DC cable system for temporary overvoltages by testing with very long impulse waveforms, *CIGRE General Meeting*, (2018). Paris, France, Aug.
- [10] Recommendations for testing DC extruded cable systems for power transmission at a rated voltage up to 500 kV, (2012). *CIGRE Tech. Rep.* 496 (WG B1.31)
- [11] IEC 62895, High voltage direct current (HVDC) power transmission - Cables with extruded insulation and their accessories for rated voltages up to 320 kV for land applications - Test methods and requirements, Dec. 2017.
- [12] M. Goertz, S. Wenig, C. Hirsching, K.M. Schäfer, S. Beckler, J. Reisbeck, M. Kahl, M. Suriyah, T. Leibfried, Overvoltage Characteristics in Symmetrical Monopole HB MMC-HVDC Configuration comprising Long Cable Systems, *Int. Conf. on Power System Transients (IPST'19)*, (2019). Perpignan, France, June
- [13] M. Goertz, S. Wenig, S. Beckler, C. Hirsching, M. Suriyah, T. Leibfried, Analysis of cable overvoltages in symmetrical monopolar and rigid bipolar HVDC configuration, *IEEE Trans. Power Del.* (2019) 1, <https://doi.org/10.1109/TPWRD.2019.2960851>.
- [14] 50Hertz Transmission GmbH Amprion GmbH, Tennet TSO GmbH, and TransnetBW GmbH, (2019). *Technical Report, German Transmission System Operators*
- [15] IEC TR 60071-4, Insulation co-ordination- Part 4: Computational guide to insulation co-ordination and modelling of electrical networks, First edition, Apr. 2004.
- [16] A. Morched, B. Gustavsen, M. Tartibi, A universal model for accurate calculation of electromagnetic transients on overhead lines and underground cables, *IEEE Trans. Power Del.* 14 (3) (1999) 1032–1038.
- [17] Guide for the development of models for HVDC converters in a HVDC grid, *CIGRE Tech. Rep.* 604 (WG B4.57)(2014).
- [18] Recommendations to improve HVDC cable systems reliability, Joint ENTSO-E and EUROPACABLE paper, www.entsoe.eu (June, 2019).
- [19] IEC 60060-1, High-voltage test techniques - Part 1: General definitions and test requirements, Nov. 2010.
- [20] M. Goertz, S. Wenig, S. Suriyah, T. Leibfried, Determination of transient overvoltages in a bipolar MMC-HVDC link with metallic return, *Proc. Power Sys. Computation Conf. Dublin, Ireland*, June 2018(2018).
- [21] Protection and local control of HVDC grids, *CIGRE Tech. Rep.* 739 (WG B4/B5.59) (2018).
- [22] IEC 60071-1, Insulation co-ordination - Part 1: Definitions, principles and rules, Aug. 2019.
- [23] IEC 60071-5, Insulation co-ordination - Part 5: Procedures for high-voltage direct current (HVDC) converter stations, Oct. 2014.
- [24] IEC 60071-2, Insulation co-ordination - Part 2: Application guidelines, Mar. 2018.
- [25] T.V. Gomes, M.A.O. Schroeder, R. Alipio, A.C.S. de Lima, A. Piantini, Investigation of overvoltages in HV underground sections caused by direct strokes considering the frequency-dependent characteristics of grounding, *IEEE Trans. Electromagn. Compat.* 60 (6) (2018) 2002–2010, <https://doi.org/10.1109/temc.2018.2798291>.
- [26] M. Goertz, S. Wenig, C. Hirsching, M. Kahl, M. Suriyah, T. Leibfried, Analysis of extruded HVDC cable systems exposed to lightning strokes, *IEEE Trans. Power Del.* 33 (6) (2018) 3009–3018, <https://doi.org/10.1109/tpwr.2018.2858569>.